Origin Invariant Molecular Orbital Decomposition of Optical Rotation

Ty Balduf[1, a)] and Marco Caricato[1, b)]
Department of Chemistry, University of Kansas, 1567 Irving Hill Road, Lawrence, Kansas 66045, United States

Optical rotation (OR) is a sensitive electronic property for which there are no clear structure-property relations. We proposed an approach to decompose the OR tensor in terms of one-electron transitions between occupied-virtual molecular orbital pairs, called the $\tilde{S}_{ia}$ method. This method allows to select the transitions with the largest magnitude that determine the overall value of the OR for a specific molecule, thus providing useful insights for characterization. However, the individual $\tilde{S}_{ia}$ values are origin-dependent even if the total OR is origin invariant. In this work, we explicitly identify the reason for the origin dependence of the $\tilde{S}_{ia}$ original formulations and we propose two ways to eliminate this spurious effect and define an origin invariant $\tilde{S}_{ia}$ within the modified velocity gauge formalism. One approach is based on averaging the electric and magnetic-perturbed density $\tilde{S}_{ia}$ definitions (which have equal and opposite origin dependence that cancels out in the average), while the second approach is based on the equal distribution of the electronic response to an external field via Cholesky decomposition of the response matrix. Numerical results prove that the new $\tilde{S}_{ia}$ definitions are indeed origin invariant and they provide the same physical picture for the OR tensor decomposition. At the same time, we show that setting the origin of the coordinate system at the center of mass of the molecule also provides the same physical picture when using the original $\tilde{S}_{ia}$ formulation, which confirms that this is a robust approach for investigating structure-property relations in chiral molecules.

Keywords: Optical Rotation, Gauge Dependence, Response Theory, Orbital Decomposition

I. INTRODUCTION

Optical rotation (OR) measurements are a common method to characterize chiral systems, but it has proven challenging to establish a chemically intuitive connection between the structure of a molecule and the OR direction or magnitude it induces. With the advent of quantum mechanical simulations of OR, significant efforts have been made to clarify this structure-property relationship. One avenue of research has focused on developing methods to decompose the OR into contributions from functional groups, bonds, or even individual atoms within the molecule[1–6].

We have recently developed a scheme, referred to as $\tilde{S}_{ia}$ analysis, whereby the OR is expressed as a sum of contributions from occupied i to virtual a molecular orbital (MO) transitions.[1] We can determine what physically is driving optical activity and what parts of the molecule are involved by analyzing the movement of charge density described by these transitions. Using this framework, we have investigated the influence of molecular conformation and functionalization on the OR induced by chiral organic molecules.[7] More recently, we used this approach to understand the origin of the large specific rotation in helicenes, and how functionalization affects the optical response.[8] We found that the major contributions come from transitions where density moves along the conjugated π density. However, other transitions, which can be described as the combination of two separate rotations of the orbital density along the two-halves of the helix, tend to decrease the OR. Functionalization of the helicenes influences the OR in a complex manner, where the strength of the substituent groups and the length of the helix may lead to cooperative or competitive effects that are not easily predicted a priori, but can be interpreted with our decomposition approach. As we showed in Ref. 9, the method is robust, providing a consistent physical interpretation of the OR in both modified velocity gauge (MVG)[10] and length gauge (LG) calculations, regardless of the choice of perturbation used in solving the linear response equations. The definition of $\tilde{S}_{ia}$ is not limited to canonical orbitals, but localized orbitals can be employed as well.[8] Since the localization procedure is essentially free in terms of computational cost, one can perform the $\tilde{S}_{ia}$ analysis with multiple MO bases simultaneously and utilize the basis with the most compact representation of the OR tensor *a posteriori*.

However, while both MVG and LG calculations of the total OR are (or can be made)[10,11] origin invariant, this does not necessarily ensure that individual $\tilde{S}_{ia}$ values will be origin invariant. The total OR is in general made origin invariant via cancellation, rather than elimination, of the origin dependent terms from each $\tilde{S}_{ia}$ value. It is possible that choosing a physically meaningful origin like the center of mass may produce reasonable $\tilde{S}_{ia}$ values, though this is not guaranteed; e.g. typical LG CCSD calculations of the total OR are origin dependent and using the center of mass as the origin does not consistently lead to high accuracy in comparison with experiment[12]. In any case, the reliability of the physical interpretations provided by the $\tilde{S}_{ia}$ analysis would be greatly improved by removing this origin dependence altogether.

In this article, we present two possible approaches to compute origin invariant $\tilde{S}_{ia}$ values in the modified velocity gauge. Section II contains a brief review of the theory

a) Electronic mail: tybalduf@ku.edu
b) Electronic mail: mcaricato@ku.edu

behind the $\tilde{S}_{ia}$ analysis and the derivation of the origin invariant formulations. The first of these procedures uses an average of the $\tilde{S}_{ia}$ values obtained from MVG electric and magnetic perturbation calculations. The second approach involves splitting the response matrix in order to form "hemi-perturbed densities" that are then contracted to form $\tilde{S}_{ia}$ values. Section III describes the computational procedure for the test calculations. In Section IV, we demonstrate that both approaches are indeed origin invariant and we compare the results with standard $\tilde{S}_{ia}$ formulations by performing calculations on two small organic molecules, P-(2,3)-pentadiene and (R)-3-chloro-1-butene. We conclude with a discussion of the relative merits of these two approaches in Section V.

II. THEORY

For isotropic media, the observed optical rotation is commonly reported as a normalized quantity in units of deg [dm (g/mL)]$^{-1}$, known as specific rotation[13]

$$[\alpha]_\omega = \frac{(72\times10^6)\hbar^2 N_A \omega^2}{3c^2 m_e^2 M}\mathrm{Tr}(\boldsymbol{\beta}) \tag{1}$$

where $\hbar$ is the reduced Planck's constant (J s), N_A is Avogadro's number, c is the speed of light (m/s), m_e is the electron rest mass (kg), and M is the molecular mass (amu). The $\boldsymbol{\beta}$ tensor is the electric dipole-magnetic dipole polarizability, which can be written in the velocity gauge as

$$\beta^V_{\alpha\beta} = \frac{2}{\omega}\sum_{j\neq0}\mathrm{Re}\frac{\langle\psi_0|\mu^V_\alpha|\psi_j\rangle\langle\psi_j|m_\beta|\psi_0\rangle}{\omega_j^2-\omega^2} = \mathrm{Re}\langle\!\langle \mu^V_\alpha; m_\beta\rangle\!\rangle_\omega \tag{2}$$

where $\boldsymbol{\mu}^V = -\boldsymbol{p}$ is the electric dipole operator in the velocity gauge and $\boldsymbol{m} = -\frac{1}{2}(\boldsymbol{r}\times\boldsymbol{p})$ is the magnetic dipole operator. Greek indices denote Cartesian coordinates, ω is the frequency of the incident electromagnetic radiation while $|\psi_j\rangle$ and ω_j are the j^{th} excited state wave function and excitation frequency, respectively. Throughout, we use atomic units unless otherwise specified and denote tensors over Cartesian indices using bold font and matrices over an orbital basis with an underline. This definition is valid for non-resonant optical activity ($\omega_j \not\approx \omega$) calculations; resonant optical activity is discussed in greater detail elsewhere.[13–16]

The sum-over-states expression for the $\boldsymbol{\beta}$ tensor in Eq. 2 is impractical for real calculations because the series is slowly converging and it requires the evaluations of hundreds of excited states.[17,18] Therefore, this tensor is efficiently evaluated through linear response theory as[19–21]

$$\beta_{\alpha\beta} = \frac{1}{\omega^2}\left[\underline{\mu}^{V\dagger}_\alpha \underline{D}^\omega \underline{m}_\beta - \underline{\mu}^{V\dagger}_\alpha \underline{D}^0 \underline{m}_\beta\right] \tag{3}$$

where $\underline{\mu}^V_\alpha$ and $\underline{m}_\beta$ are respectively the α and β Cartesian components of the velocity gauge electric and magnetic dipoles, represented as vectors over all orbital pairs in the given basis. $\underline{D}^\omega = \underline{\Omega}^{-1}$ is the linear response matrix for the perturbation frequency ω and $\underline{D}^0$ is the zero frequency response matrix. The second term in Eq. 3 is the spurious static limit that must be subtracted out in the velocity gauge.[10] For a general self consistent field (SCF) wavefunction, we can write the matrix elements more explicitly as

$$\underline{D}^\omega = \left[\begin{pmatrix}\underline{M} & \underline{Q}\\ \underline{Q}^* & \underline{M}^*\end{pmatrix} - \omega\begin{pmatrix}\underline{1} & \underline{0}\\ \underline{0} & -\underline{1}\end{pmatrix}\right]^{-1} \tag{4}$$

$$Q_{ai,bj} = (ai|bj) - c_{\mathrm{HF}}(aj|bi) + (ai|v_{xc}|bj) \tag{5}$$

$$M_{ai,bj} = \delta_{ij}\delta_{ab}(\epsilon_a-\epsilon_i) + (ai|jb) - c_{\mathrm{HF}}(ab|ji) + (ai|v_{xc}|jb) \tag{6}$$

with i,j denoting occupied orbitals and a,b denoting virtual orbitals, v_{xc} is the exchange-correlation kernel (0 in the case of HF), and c_{HF} is the percentage of Hartree-Fock exchange[21–24].

As mentioned above, for experiments in isotropic media, the observed optical rotation is proportional to the trace of $\boldsymbol{\beta}$, see Eq. 1. We can gain insight into what underlying physical processes are contributing to this trace by splitting it into contributions from orbital pairs, referred to as $\tilde{S}_{ia}$ values[9]

$$\tilde{S}^{\mathrm{M},\omega}_{ia} = \frac{1}{\omega}\sum_\alpha\sum_{jb}\langle\phi_i|\mu^V_\alpha|\phi_a\rangle\left(D^\omega_{ia,jb}\langle\phi_b|m_\alpha|\phi_j\rangle\right) \tag{7a}$$

$$= \frac{1}{\omega}\boldsymbol{\mu}_{ia}\cdot\boldsymbol{P}^{\mathrm{M},\omega}_{ia} \tag{7b}$$

$$\tilde{S}^{\mathrm{E},\omega}_{ia} = \frac{1}{\omega}\sum_\alpha\sum_{jb}\langle\phi_i|m_\alpha|\phi_a\rangle\left(D^\omega_{ia,jb}\langle\phi_b|\mu^V_\alpha|\phi_j\rangle\right) \tag{7c}$$

$$= \frac{1}{\omega}\boldsymbol{m}_{ia}\cdot\boldsymbol{P}^{\mathrm{E},\omega}_{ia} \tag{7d}$$

With these definitions, the trace of $\boldsymbol{\beta}$ is recovered as

$$\begin{aligned}\mathrm{Tr}(\boldsymbol{\beta}) &= \frac{1}{\omega}\sum_{ia}\tilde{S}^{\mathrm{M},\omega}_{ia} - \tilde{S}^{\mathrm{M},0}_{ia} = \frac{1}{\omega}\sum_{ia}\tilde{S}^{\text{MVG-M}}_{ia}\\ &= \frac{1}{\omega}\sum_{ia}\tilde{S}^{\mathrm{E},\omega}_{ia} - \tilde{S}^{\mathrm{E},0}_{ia} = \frac{1}{\omega}\sum_{ia}\tilde{S}^{\text{MVG-E}}_{ia}\end{aligned} \tag{8}$$

The difference between the two definitions is based on which integrals are contracted first with the response matrix: In Eq. 7a, the response matrix is contracted with the magnetic dipole integrals (MVG-M) to form the perturbed density $\boldsymbol{P}^{M,\omega}_{ia}$ in Eq. 7b; conversely, in Eq. 7c, the response matrix is contracted with the electric dipole integrals (MVG-E) to form the perturbed density $\boldsymbol{P}^{E,\omega}_{ia}$ in Eq. 7d. The expressions for the static frequency $\tilde{S}^0_{ia}$ are the same, but with $\underline{D}^\omega$ replaced by $\underline{D}^0$ (the leading factor of ω is retained). Eq. 7 is equivalent to the expressions for MVG-M and MVG-E in Eq. 8 of Ref. 9; we write them here in terms of the response matrix as this makes it easier to present how the origin dependence emerges (and can be removed). We have previously shown that, in general, $\tilde{S}^{\text{MVG-M}}_{ia} \neq \tilde{S}^{\text{MVG-E}}_{ia}$; however, the $\tilde{S}_{ia}$ values for

each choice of perturbation are associated with the same physical process and the relative contribution of this process to the observed OR is roughly the same[9]. A feature of the $\tilde{S}_{ia}$ definition in Eq. 7 is that its values can be visualized as the dot product of two vectors that represent charge transfer ($\boldsymbol{\mu}$) and charge rotation ($\boldsymbol{m}$). These vectors can be visualized and superimposed to the molecular structure to determine what types of one-electron (1e) transition contribute the most to the OR.[1,7–9] This vector analysis holds for the MVG approach because one can define an MVG perturbed density vector that is dotted with the vector of the paired perturbation

$$\tilde{S}_{ia}^{\mathrm{M},\omega} - \tilde{S}_{ia}^{\mathrm{M},0} = \frac{1}{\omega}\boldsymbol{\mu}_{ia}^{V} \cdot (\boldsymbol{P}_{ia}^{\mathrm{M},\omega} - \boldsymbol{P}_{ia}^{\mathrm{M},0}) \tag{9}$$

$$\tilde{S}_{ia}^{\mathrm{E},\omega} - \tilde{S}_{ia}^{\mathrm{E},0} = \frac{1}{\omega}\boldsymbol{m}_{ia} \cdot (\boldsymbol{P}_{ia}^{\mathrm{E},\omega} - \boldsymbol{P}_{ia}^{\mathrm{E},0}) \tag{10}$$

While the total OR computed in the modified velocity gauge is origin invariant regardless of the perturbation used, this is not the case for the individual $\tilde{S}_{ia}$ values, even in the limit of an exact calculation using a complete basis set. The origin dependence of $\tilde{S}_{ia}$ for each choice of perturbation follows directly from that of the full $\boldsymbol{\beta}$ tensor, which is detailed for instance in Refs. 11,25,26. For a shifted origin $\boldsymbol{O'} = \boldsymbol{O} + \boldsymbol{d}$, displaced by a vector $\boldsymbol{d}$, the $\tilde{S}_{ia}$ origin dependence can be expressed as

$$\begin{aligned}\tilde{S}_{ia}^{\mathrm{M},\omega}(\boldsymbol{O'}) =& \frac{1}{\omega}\sum_{\alpha}\sum_{jb}\langle\phi_i|\mu_\alpha^V|\phi_a\rangle D_{ia,jb}^{\omega}\Big(\langle\phi_b|m_\alpha|\phi_j\rangle \\ &- \sum_{\beta\gamma}\epsilon_{\alpha\beta\gamma}\langle\phi_b|\mu_\beta^V|\phi_j\rangle d_\gamma\Big) \\ =& \tilde{S}_{ia}^{\mathrm{M},\omega}(\boldsymbol{O}) - \frac{\omega}{2}\sum_{\alpha\beta\gamma}\epsilon_{\alpha\beta\gamma}\alpha_{\alpha\beta,ia}^{V,\omega}d_\gamma \end{aligned} \tag{11a}$$

$$\begin{aligned}\tilde{S}_{ia}^{\mathrm{E},\omega}(\boldsymbol{O'}) =& \frac{1}{\omega}\sum_{\alpha}\sum_{jb}\Big(\langle\phi_i|m_\alpha|\phi_a\rangle \\ &- \sum_{\beta\gamma}\epsilon_{\alpha\beta\gamma}\langle\phi_i|\mu_\beta^V|\phi_a\rangle d_\gamma\Big)D_{ia,jb}^{\omega}\langle\phi_b|\mu_\alpha^V|\phi_j\rangle \\ =& \tilde{S}_{ia}^{\mathrm{E},\omega}(\boldsymbol{O}) + \frac{\omega}{2}\sum_{\alpha\beta\gamma}\epsilon_{\alpha\beta\gamma}\alpha_{\alpha\beta,ia}^{V,\omega}d_\gamma \end{aligned} \tag{11b}$$

where $\boldsymbol{\epsilon}$ is the Levi-Civita symbol, $\boldsymbol{\alpha^V}$ is the velocity gauge electric dipole-electric dipole polarizability. The origin dependence for each choice of perturbation comes from differences between the off-diagonal elements of $\boldsymbol{\alpha}_{ia}^{V}$; the total MVG $\boldsymbol{\alpha}$ is symmetric, so these terms cancel out when summing over all occupied-virtual orbital pairs, but each $\boldsymbol{\alpha}_{ia}^{V}$ is in general not symmetric.

The form of Eqs. 11a and 11b suggests a simple approach for eliminating origin dependence from $\tilde{S}_{ia}$:

$$\tilde{S}_{ia}^{\mathrm{Avg}} = \frac{1}{2}\big(\tilde{S}_{ia}^{\text{MVG-M}} + \tilde{S}_{ia}^{\text{MVG-E}}\big) \tag{12}$$

Since the origin dependent terms for $\tilde{S}_{ia}^{\text{MVG-M}}$ and $\tilde{S}_{ia}^{\text{MVG-E}}$ are equal in magnitude but opposite in sign, they cancel in the average, leaving $\tilde{S}_{ia}^{\mathrm{Avg}}$ origin invariant. $\tilde{S}_{ia}^{\mathrm{Avg}}$ still satisfies Eq. 8, which means it can still be used as an interpretive tool to understand which occupied to virtual orbital transitions are driving the OR. However, while $\tilde{S}_{ia}^{\text{MVG-M}}$ and $\tilde{S}_{ia}^{\text{MVG-E}}$ each have associated electric/magnetic dipole and perturbed density vectors describing the flow of charge during the $i \to a$ transition, see Eq. 9, $\tilde{S}_{ia}^{\mathrm{Avg}}$ does not have an associated set of vectors. This is because simply averaging the MVG-M and MVG-E electric/magnetic vectors and taking their dot product is not equivalent to averaging the MVG-M and MVG-E dot products from Eqs. 7b and d, as is done in Eq. 12.

An alternative approach to removing the origin dependence involves mixing the electric and magnetic response prior to forming $\tilde{S}_{ia}$. The origin dependence stems from the asymmetry of $\boldsymbol{\alpha}_{ia}^{V}$, so one can reformulate the electronic response such that the resulting $\tilde{\boldsymbol{\alpha}}_{ia}^{V}$ is symmetric for every occupied-virtual orbital pair. This can be achieved via Cholesky decomposition[27] of the response matrix

$$\underline{D}^{\omega} = \underline{L}^{\omega}\underline{L}^{\omega\dagger} \tag{13}$$

where $\underline{L}^{\omega}$ is a lower triangular square matrix with all positive real values along its diagonal. Note that we are not using the Cholesky decomposition to lower the rank of a tensor, as it is usually employed in electronic structure methods, but simply to "evenly distribute" the response matrix to both perturbations. By splitting the response matrix, we can apply $\underline{L}^{\omega}$ to both the electric dipole and magnetic dipole to obtain "hemi-perturbed" densities and contract these to form

$$\tilde{S}_{ia}^{\mathrm{Hemi},\omega} = \frac{1}{\omega}\sum_{\alpha}\sum_{jb}(L_{ia,jb}^{\omega}\langle\phi_j|\mu_\alpha^V|\phi_b\rangle)(L_{ia,jb}^{\omega}\langle\phi_b|m_\alpha|\phi_j\rangle) \tag{14}$$

To see that this formulation of $\tilde{S}_{ia}$ is origin invariant, we simply need to show that the corresponding electric dipole polarizability

$$\alpha_{\alpha\beta,ia}^{\mathrm{Hemi},\omega} = \frac{1}{\omega}\sum_{jb}(L_{ia,jb}^{\omega}\langle\phi_j|\mu_\alpha^V|\phi_b\rangle)(L_{ia,jb}^{\omega}\langle\phi_b|\mu_\beta^V|\phi_j\rangle) \tag{15}$$

is symmetric, which is evident since it is formed from the contraction of a vector with itself.

However, this method also does not allow us to assign unique electric and magnetic vectors to each transition as in Eq. 9. The reason is that for MVG, this approach leads to an electric and magnetic hemi-density both for the applied perturbation frequency and the static frequency. Simply taking the difference of both perturbed and static electric/magnetic hemi-densities and contracting them does not produce the same product as Eq. 15. Another potential issue of this hemi-density approach is that the Cholesky decomposition is only possible for Hermitian, positive-semidefinite matrices (i.e. matrices with only real eigenvalues greater than or equal to 0). While

the response matrix is always Hermitian, it is only required to be positive-definite in the static limit[21,28]. This method would also require extensive updates to the typical linear response implementation, as generally the response matrix is not formed explicitly, but rather the perturbed density is formed through an iterative process.[22] Therefore, we implemented it only as an external Python script.

A third possibility to obtain individually origin-invariant $\tilde{S}_{ia}$ values is to perform a singular value decomposition (SVD) of each $\boldsymbol{\alpha}^V_{ia}$ tensor, to form individual $\boldsymbol{\beta}^V_{ia}$ tensors for each ia MO pairs, and to apply the inverse SVD transformation to the $\boldsymbol{\beta}^V_{ia}$ tensors. The inverse SVD transformation would render the $\boldsymbol{\alpha}^V_{ia}$ tensors diagonal and it would eliminate the origin dependence of the $\tilde{S}_{ia}$ terms in Eq. 11. This transformation would be analogous to that to obtain origin-invariant length gauge OR without using London orbitals, LG(OI),[11,26,29,30] and LG(OI) rotatory strengths for electronic transitions.[31] However, in Ref. 31 it was shown that applying this transformation to individual rotatory strengths disrupts the sum-over-state relationship between these quantities and the overall OR, i.e., the equivalent of Eq. 2 for the length gauge, where the rotatory strengths are the numerators. In the context of the $\tilde{S}_{ia}$ approach, where these quantities can be considered rotatory strengths in the space of Slater determinants rather than eigenstates of the Hamiltonian,[1] applying the SVD transformation to individual $\tilde{S}_{ia}$ would disrupt the equality in Eq. 8. Therefore, we do not pursue this route further.

III. COMPUTATIONAL DETAILS

We performed Hartree-Fock (HF) calculations with the aug-cc-pVDZ basis set[32] with a 589.3 nm perturbation wavelength to avoid resonance conditions. It is not our intention to compute experimentally accurate OR, but rather simply to demonstrate the origin invariance of the $\tilde{S}^{\text{Avg}}_{ia}$ and $\tilde{S}^{\text{Hemi}}_{ia}$ definitions, see Eqs. 12 and 14, respectively. Furthermore, the implementation of the $\tilde{S}^{\text{Hemi}}_{ia}$ definition is based on a simple Python code that forms the entire response matrix in Eq. 4, then applies the Cholesky decomposition in Eq. 13 to form $\tilde{S}^{\text{Hemi}}_{ia}$. The Python code reads two-electron integrals and orbital energies from a modified version of the GAUSSIAN suite of programs[33] to form the appropriate matrices and it is very time and memory intensive. Consequently, calculations are performed at HF (rather than density functional theory) level to avoid the need to also read in 4-center, 1-electron exchange-correlation integrals when computing $\tilde{S}^{\text{Hemi}}_{ia}$. However, the results obtained here equally apply to calculations using approximate density functionals. All OR and $\tilde{S}^{\text{Avg}}_{ia}$ calculations were performed with the same development version of GAUSSIAN[33].

IV. RESULTS

We consider two small molecules, P-(2,3)-pentadiene (hereafter pentadiene) and (R)-3-chloro-1-butene (hereafter chlorobutene), to compare $\tilde{S}^{\text{Avg}}_{ia}$ and $\tilde{S}^{\text{Hemi}}_{ia}$ with the origin dependent $\tilde{S}^{\text{MVG-M}}_{ia}$ and $\tilde{S}^{\text{MVG-E}}_{ia}$. The geometry for pentadiene was taken from Ref. 6 while chlorobutene was optimized at the B3LYP/aug-cc-pVDZ level; these geometries are reported in Tables S1-S2 of the SI. This comparison will help to determine if there are any differences in the physical interpretation of the OR suggested by each method. Figures 1 and 2 plot $\tilde{S}_{ia}$ values for the 20 highest occupied and 20 lowest virtual MOs of pentadiene and chlorobutene computed with each of the definitions of $\tilde{S}_{ia}$ discussed in Section II. To demonstrate the origin independence of the $\tilde{S}^{\text{Avg}}_{ia}$ and $\tilde{S}^{\text{Hemi}}_{ia}$ approaches, we plot the results of calculations with the origin at the center of mass (COM) of the molecule and with the origin shifted by -100Å in each Cartesian direction from the COM.

Starting first with the COM plots, we can see that for each molecule the distribution of contributions is very similar for each of the definitions of $\tilde{S}_{ia}$. For pentadiene, the largest negative contribution is from the (HOMO-1, LUMO+12) transition and the largest positive contribution is from the (HOMO, LUMO+14) transition for each of the definitions. Chlorobutene has a larger number of significant contributions that maintain the same sign across definitions and the largest magnitude contributions are consistently from a small band of 3 transitions from (HOMO, LUMO+7) to (HOMO, LUMO+9). These five largest values of $\tilde{S}_{ia}$ for the two molecules are shown in Figure 3. The relative magnitude is respected across different definitions of $\tilde{S}_{ia}$, although $\tilde{S}^{\text{Hemi}}_{ia}$ provides value that are larger in magnitude for these prominent transitions (which is compensated by the remaining smaller values as their total sum adds up to the trace of the $\boldsymbol{\beta}$ tensor). The $\tilde{S}^{\text{MVG-M}}_{ia}$ and $\tilde{S}^{\text{MVG-E}}_{ia}$ distributions closely match the origin invariant $\tilde{S}^{\text{Avg}}_{ia}$ and $\tilde{S}^{\text{Hemi}}_{ia}$ distributions, which suggests that the center of mass is a reasonable choice of origin.

In the shifted-origin plots for each molecule, while the $\tilde{S}^{\text{Avg}}_{ia}$ and $\tilde{S}^{\text{Hemi}}_{ia}$ results are identical to those computed with the COM origin (within numerical accuracy), the origin-dependent terms of $\tilde{S}^{\text{MVG-M}}_{ia}$ and $\tilde{S}^{\text{MVG-E}}_{ia}$ dominate the shifted-origin plots. The difference in sign between the origin dependent terms of $\tilde{S}^{\text{MVG-M}}_{ia}$ and $\tilde{S}^{\text{MVG-E}}_{ia}$ is clearly visible comparing the left-hand and right-hand side plots. For instance, for pentadiene, the (HOMO-1, LUMO+12) and (HOMO, LUMO+14) MVG-M transitions both changed sign relative to the COM calculation, while also increasing in magnitude by a factor of 3, exceeding the range of the COM origin color map. The $\tilde{S}^{\text{MVG-M}}_{ia}$ values for the (HOMO-1, LUMO+10) and (HOMO, LUMO+11) transitions increased in size by more than an order of magnitude. For chlorobutene, many transitions increased in magnitude enough to exceed the range of the COM origin color map. The

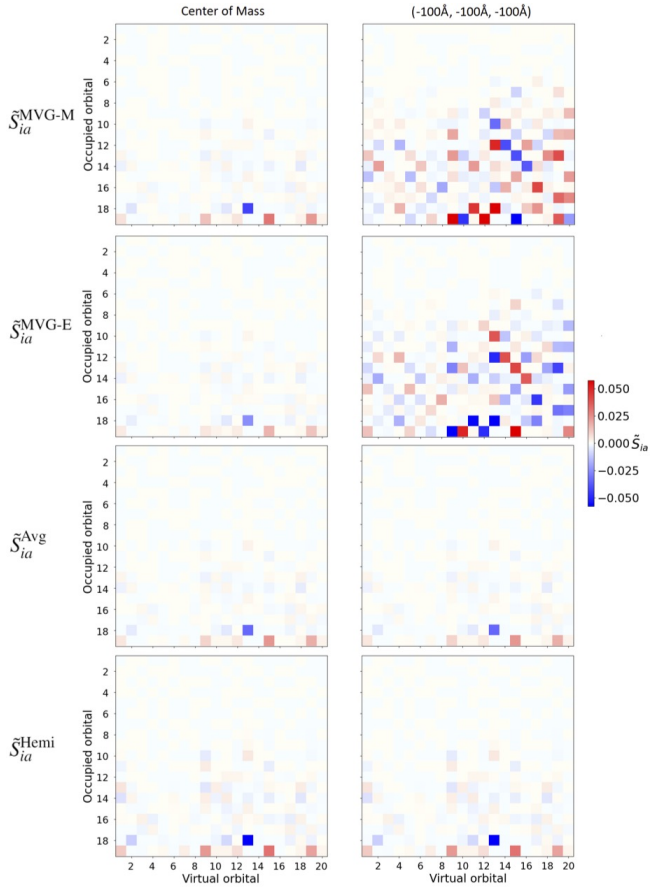

FIG. 1. $\tilde{S}_{ia}$ values for the 20 highest occupied and 20 lowest virtual MOs of P-(2,3)-pentadiene computed with (from top to bottom) the MVG-M, MVG-E, average, and hemi-density definitions of $\tilde{S}$. Results with the origin at the center of mass and shifted by -100Å in the x, y, and z directions are plotted in the left and right columns, respectively. The heat maps color range is from $-M$ to M where $M = \max(|\tilde{S}_{ia}^{X}|), X = \{\text{MVG-M, MVG-E, Avg, Hemi}\}$ for the center of mass calculations. The shifted origin heat maps use the same color range, but some $\tilde{S}_{ia}$ exceed this range and are simply colored the same as $-M/M$.

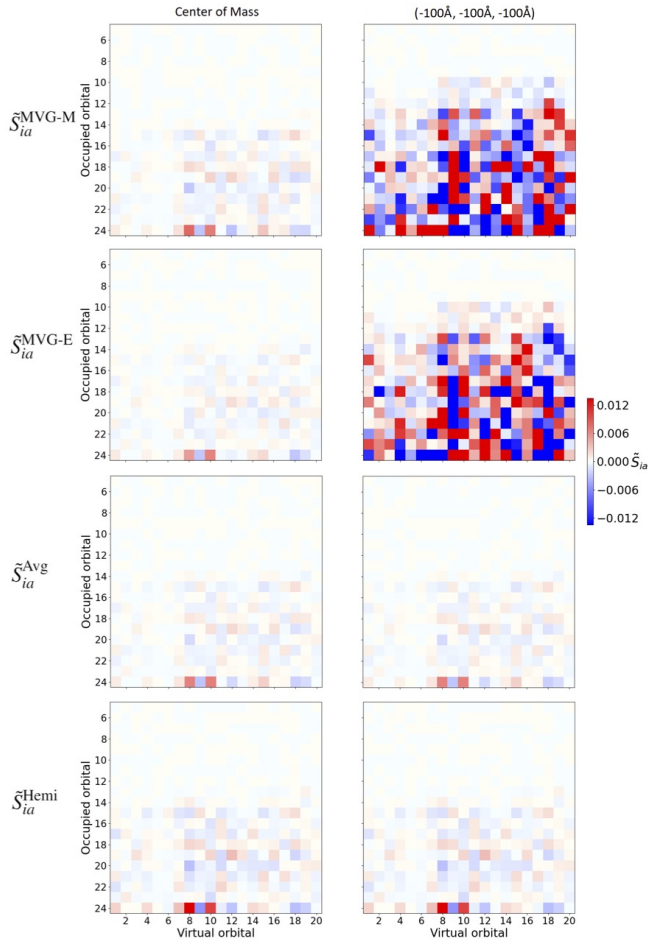

FIG. 2. $\tilde{S}_{ia}$ values for the 20 highest occupied and 20 lowest virtual MOs of (R)-3-chloro-1-butene computed with (from top to bottom) the MVG-M, MVG-E, average, and hemi-density definitions of $\tilde{S}$. Results with the origin at the center of mass and shifted by -100Å in the x, y, and z directions are plotted in the left and right columns, respectively. The heat maps color range is from $-M$ to M where $M = \max(|\tilde{S}_{ia}^{X}|), X = \{\text{MVG-M, MVG-E, Avg, Hemi}\}$ for the center of mass calculations. The shifted origin heat maps use the same color range, but some $\tilde{S}_{ia}$ exceed this range and are simply colored the same as $-M/M$.

(HOMO, LUMO+7), the largest magnitude $\tilde{S}_{ia}^{\text{MVG-M}}$ of the COM calculations, remains the largest transition in the shifted calculations, but increases in size from 7.82×10^{-3} a.u. to 2.78×10^{-1} a.u.

V. CONCLUSIONS

We have introduced two new methods for decomposing the OR into origin invariant $\tilde{S}_{ia}$ values. The $\tilde{S}_{ia}^{\text{Avg}}$ approach exploits the equal magnitude, opposite sign origin dependence of $\tilde{S}_{ia}^{\text{MVG-M}}$ and $\tilde{S}_{ia}^{\text{MVG-E}}$ to cancel out the origin dependence. For $\tilde{S}_{ia}^{\text{Hemi}}$, we contract hemi-perturbed densities formed by splitting the linear response matrix evenly between the electric and magnetic dipoles. The MVG hemi-density electric dipole-electric dipole polarizability for each transition $\boldsymbol{\alpha}_{ia}^{\text{Hemi}}$ is inherently symmetric, which eliminates the origin-dependent contribution to $\tilde{S}_{ia}$.

The tests in Figures 1-2 clearly show that these two new definitions are indeed origin invariant. More importantly, these tests show that $\tilde{S}_{ia}^{\text{Avg}}$ and $\tilde{S}_{ia}^{\text{Hemi}}$ provide the same physical picture for the decomposition of the OR in terms of ia MO pairs, i.e., the same 1e transitions contribute with the same relative magnitude and sign to the overall tensor (even if the numerical values of $\tilde{S}_{ia}^{\text{Avg}}$ and $\tilde{S}_{ia}^{\text{Hemi}}$ are different). Moreover, the results obtained at the COM origin are consistent across all definitions of $\tilde{S}_{ia}$, either in the form in Eqs. 7, 12, or 14. This indicates that setting the origin at the COM of a molecule is a

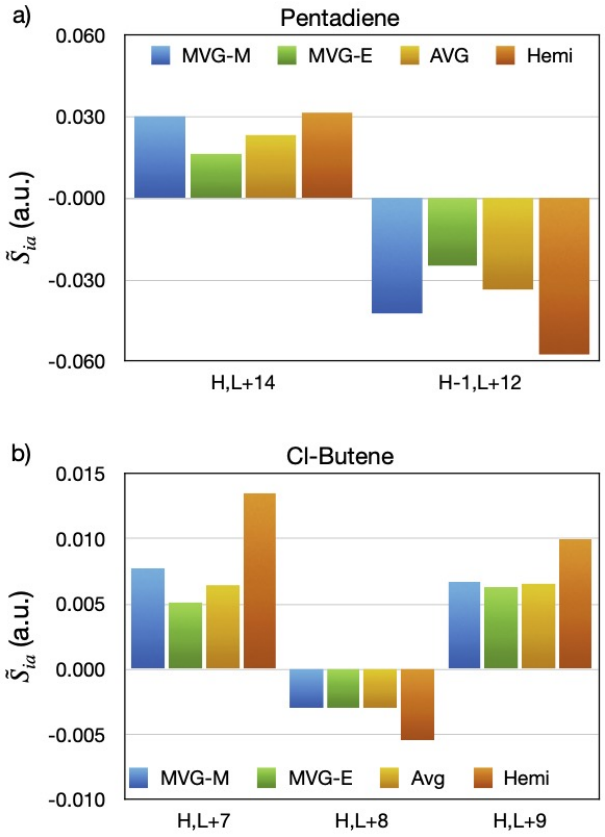

FIG. 3. Largest $\tilde{S}_{ia}$ values (a.u.) for: a) P-(2,3)-pentadiene and b) (R)-3-chloro-1-butene, computed with the MVG-M, MVG-E, average, and hemi-density definitions of $\tilde{S}$.

good choice and further confirms that this orbital decomposition of the $\boldsymbol{\beta}$ tensor is robust and can provide useful insights into the electronic and geometrical features that determine the OR of chiral molecules.

Between the two approaches, $\tilde{S}_{ia}^{\text{Hemi}}$ is computationally more demanding because it requires the evalution of the whole response matrix, see Eq. 13, at least in a straightforward application, which is memory and CPU intensive for real calculations. Furthermore, the requirement that the response matrix is positive definite cannot be guaranteed for a generic system. Therefore, the $\tilde{S}_{ia}^{\text{Avg}}$ definition is preferable because it is always well defined and computationally cheaper. A downside of both $\tilde{S}_{ia}$ definitions is that it is not straightforward to associate transition vectors to a specific value with MVG because in both cases the spurious static limit is mixed with the ω-dependent term in a non-trivial fashion. Nonetheless, these schemes provide reference values for the determination of the most important contributions to the total OR of chiral molecules that can be used to benchmark the standard $\tilde{S}_{ia}$ results computed as in Eq. 7. The latter can then be used for a detailed analysis of the electron density redistribution for these relevant transitions as done in our previous studies.[1,7–9] Further studies will investigate whether these formulations can be extended to the length gauge approach, which does not have the spurious static limit issue but where the whole tensor is origin dependent.[11,29]

SUPPORTING INFORMATION

The Supporting Information includes the geometries for P-(2,3)-pentadiene and (R)-3-chlorobutene in Tables S1-S2.

ACKNOWLEDGMENTS

The authors gratefully acknowledge support from the National Science Foundation through Grant No. CHE-1650942.

[1] Caricato M (2015) Orbital analysis of molecular optical activity based on configuration rotatory strength. J Chem Theory Comput 11(4):1349–1353. doi:10.1021/acs.jctc.5b00051
[2] Kirkwood JG (1937) On the theory of optical rotatory power. J Chem Phys 5(6):479. doi:10.1063/1.1750060
[3] Kondru RK, Wipf P, Beratan DN (1998) Atomic contributions to the optical rotation angle as a quantitative probe of molecular chirality. Science 282(5397):2247–2250. doi:10.1126/science.282.5397.2247
[4] Moore B, Srebro M, Autschbach J (2012) Analysis of optical activity in terms of bonds and lone-pairs: The exceptionally large optical rotation of norbornenone. J Chem Theory Comput 8(11):4336–4346. doi:10.1021/ct300839y
[5] Polavarapu PL, Chakraborty DK, Ruud K (2000) Molecular optical rotation: An evaluation of semiempirical models. Chem Phys Lett 319(5):595–600. doi:10.1016/S0009-2614(00)00157-3
[6] Wiberg KB, Caricato M, Wang YG, et al (2013) Towards the accurate and efficient calculation of optical rotatory dispersion using augmented minimal basis sets. Chirality 25(10):606–616. doi:10.1002/chir.22184
[7] Caricato M (2015) Conformational effects on specific rotation: A theoretical study based on the $\tilde{S}_k$ method. J Phys Chem A 119(30):8303–8310. doi:10.1021/acs.jpca.5b05103
[8] Aharon T, Caricato M (2019) Configuration space analysis of the specific rotation of helicenes. J Phys Chem A 123(20):4406–4418. doi:10.1021/acs.jpca.9b01823
[9] Balduf T, Caricato M (2021) Gauge Dependence of the $\tilde{S}$ Molecular Orbital Space Decomposition of Optical Rotation. J Phys Chem A 125(23):4976–4985. doi:10.1021/acs.jpca.1c01653
[10] Pedersen TB, Koch H, Boman L, et al (2004) Origin invariant calculation of optical rotation without recourse to London orbitals. Chem Phys Lett 393(4-6):319–326. doi:10.1016/j.cplett.2004.06.065
[11] Caricato M (2020) Origin invariant optical rotation in the length dipole gauge without London atomic orbitals. J Chem Phys 153(15):151,101. doi:10.1063/5.0028849
[12] Crawford TD, Stephens PJ (2008) Comparison of Time-Dependent Density-Functional Theory and Coupled Cluster Theory for the Calculation of the Optical Rotations of Chiral Molecules. J Phys Chem A 112(6):1339–1345. doi:10.1021/jp0774488
[13] Barron LD (2004) Molecular Light Scattering and Optical Activity. Cambridge University Press, Cambridge, UK; New York
[14] Buckingham AD, Dunn MB (1971) Optical activity of oriented molecules. J Chem Soc Inorg Phys Theor Chem (0):1988–1991. doi:10.1039/J19710001988
[15] Krykunov M, Autschbach J (2006) Calculation of origin-independent optical rotation tensor components in approxi-

mate time-dependent density functional theory. J Chem Phys 125:034,102. doi:10.1063/1.2210474

[16]Norman P, Ruud K, Helgaker T (2004) Density-functional theory calculations of optical rotatory dispersion in the nonresonant and resonant frequency regions. J Chem Phys 120(11):5027–5035. doi:10.1063/1.1647515

[17]Wiberg KB, Wang YG, Wilson SM, et al (2006) Sum-over-states calculation of the specific rotations of some substituted oxiranes, chloropropionitrile, ethane, and norbornenone. J Phys Chem A 110(51):13,995–14,002. doi:10.1021/jp0655221

[18]Caricato M, Vaccaro PH, Crawford TD, et al (2014) Insights on the Origin of the Unusually Large Specific Rotation of (1*S*,4*S*)-Norbornenone. J Phys Chem A 118(26):4863–4871. doi:10.1021/jp504345g

[19]Autschbach J, Nitsch-Velasquez L, Rudolph M (2011) Time-dependent density functional response theory for electronic chiroptical properties of chiral molecules. Top Curr Chem 298:1–98. doi:10.1007/128_2010_72

[20]Crawford TD, Tam MC, Abrams ML (2007) The current state of ab initio calculations of optical rotation and electronic circular dichroism spectra. J Phys Chem A 111(48):12,057–12,068. doi:10.1021/jp075046u

[21]McWeeny R (1978) Methods of Molecular Quantum Mechanics, 2nd edn. Academic Press, San Diego

[22]Frisch M, Head-Gordon M, Pople J (1990) Direct analytic SCF second derivatives and electric field properties. Chem Phys 141(2-3):189–196. doi:10.1016/0301-0104(90)87055-G

[23]Izmaylov AF, Brothers EN, Scuseria GE (2006) Linear-scaling calculation of static and dynamic polarizabilities in Hartree-Fock and density functional theory for periodic systems. J Chem Phys 125(22):224,105. doi:10.1063/1.2404667

[24]Pople JA, Krishnan R, Schlegel HB, et al (1979) Derivative Studies in Hartree-Fock and Moller-Plesset Theories. Int J Quantum Chem 13:225–241

[25]Lazzeretti P (2014) Invariance of Molecular Response Properties under a Coordinate Translation. Int J Quantum Chem 114:1364–1392

[26]Caricato M, Balduf T (2021) Origin invariant full optical rotation tensor in the length dipole gauge without London atomic orbitals. J Chem Phys 155(2):024,118. doi:10.1063/5.0053450

[27]Aquilante F, Boman L, Boström J, et al (2011) Cholesky Decomposition Techniques in Electronic Structure Theory. In: Zalesny R, Papadopoulos MG, Mezey PG, et al (eds) Linear-Scaling Techniques in Computational Chemistry and Physics, vol 13. Springer Netherlands, Dordrecht, p 301–343, doi:10.1007/978-90-481-2853-2_13

[28]Čížek J, Paldus J (1967) Stability Conditions for the Solutions of the Hartree—Fock Equations for Atomic and Molecular Systems. Application to the Pi-Electron Model of Cyclic Polyenes. J Chem Phys 47(10):3976–3985. doi:10.1063/1.1701562

[29]Ditchfield R (1974) Self-consistent perturbation theory of diamagnetism I. A gauge-invariant LCAO method for N.M.R. Chemical shifts. Mol Phys 27(4):789–807. doi:10.1080/00268977400100711

[30]London F (1937) Théorie quantique des courants interatomiques dans les combinaisons aromatiques. J Phys Radium 8(10):397–409. doi:10.1051/jphysrad:01937008010039700

[31]Niemeyer N, Caricato M, Neugebauer J (2022) Origin invariant electronic circular dichroism in the length dipole gauge without london atomic orbitals. J Chem Phys 156(15):154,114

[32]Dunning TH (1989) Gaussian basis sets for use in correlated molecular calculations. I. The atoms boron through neon and hydrogen. J Chem Phys 90(2):1007. doi:10.1063/1.456153

[33]Frisch MJ, Trucks GW, Schlegel HB, et al (2020) Gaussian development version revision J.13